ISBN: 978-3-95450-253-0 ISSN: 2673-5571 doi:10.18429/JACoW-HB2023-TUC1I1

MULTI-BEAM OPERATION OF LANSCE ACCELERATOR FACILITY

Y. K. Batygin, Los Alamos National Laboratory, Los Alamos, NM, USA

Abstract

The Los Alamos Neutron Science Center (LANSCE) accelerator facility has been in operation for 50 years performing important scientific support for national security. The unique feature of the LANSCE accelerator facility is multi-beam operation, delivering beams to five experimental areas. The near-term plans are to replace obsolete and almost end-of-life systems of the LANSCE linear accelerator with a modern 100-MeV Front End with significant improvement in beam quality. This paper summarizes experimental results obtained during the operation of the LANSCE accelerator facility and considers plans to expand the performance of the accelerator for near- and long-term operations.

LANSCE ACCELERATOR FACILITY

The 800 MeV LANSCE accelerator (formerly known as the Los Alamos Meson Physics Facility, LAMPF) started routine operation in 1972 with an average proton beam current of 1 mA delivering 800 kW of average beam power for meson physics research and provided high-power proton beam for a quarter century [1]. Within 50 years of operation, the accelerator facility was continuously upgraded and modified to support the Laboratory's national security mission and provide needs in fundamental nuclear physics.

The layout of the existing LANSCE accelerator facility is shown schematically in Fig. 1. The accelerator is equipped with two independent injectors for H^+ and H^- beams. Each injector has a Cockcroft-Walton type generator and an ion source to produce either positively charged protons (H^+) or negatively charged hydrogen ions (H^-) with a final energy of 750 keV. Two independent beamlines deliver H^+ and H^- beams, merging at the entrance of a 201.25 MHz Drift Tube Linac (DTL). The DTL performs acceleration up to the energy of 100 MeV. After the DTL, the Transition Region beamline directs the 100 MeV proton beam to the Isotope Production Facility (IPF), while H^- beam is accelerated up to the final energy of 800 MeV in an 805 MHz Coupled Cavity Linac (CCL). The H^- beams, created with different time structures imparted by a low-energy chopper are distributed in the Switch Yard to four experimental areas: Lujan Neutron Science Center equipped with the Proton Storage Ring (PSR), Weapons Neutron Research (WNR) Facility, Proton Radiography Facility (pRad), and Ultra-Cold Neutron Facility (UCN). The accelerator operates at 120 Hz repetition rate with 625 μs pulse length. Parameters of all beams are presented in Table 1.

batygin@lanl.gov

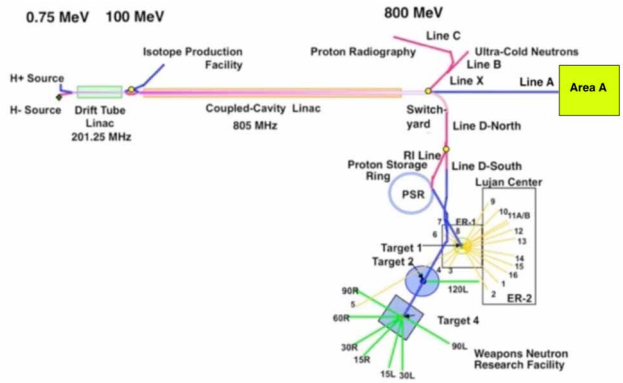

Figure 1: Overview of the LANSCE accelerator and user facility complex.

Table 1: Beam Parameters of LANSCE Accelerator

Area	Rep. Rate (Hz)	Curent/ Bunch (mA)	Average Current (μA)	Average Power (kW)
Lujan	20	10	100	80
IPF	100	4	250	25
WNR	100	25	4.5	3.6
pRad	1	10	<1	<1
UCN	20	10	10	8

BEAM TIME STRUCTURE

A unique feature of the LANSCE accelerator facility is the acceleration of four H^- beams (differing in time structure) and one H^+ beam. This is achieved by a combination of chopper and RF bunchers. Figure 2 illustrates the time structure of LANSCE beams. Figure 3 shows the time pattern of beam cycles. The H^- chopper, which creates various time structures of H^- beams, is located downstream of the H^- Cockcroft-Walton column. It consists of two traveling-wave helix electrodes, which apply a vertical kick to the beam. The chopper is normally energized so that no beam gets through. An electrical pulse of various lengths between 36 - 290 ns travels along the chopper allowing the un-chopped part of the beam pulse to pass through. The minimum width of the chopper pulse is determined by the chopper's rise time, which is about 10 ns. Following the chopper, the leading and trailing edges of the beam are bent vertically.

The Lujan Center receives 20 Hz x 625 μs pulses of H^- beam with 10 mA/bunch peak current, corresponding to an average current of 100 μA and an average beam power of 80 kW (see Fig. 3a). This beam is chopped within a time

ISBN: 978-3-95450-253-0 ISSN: 2673-5571 doi:10.18429/JACoW-HB2023-TUC1I1

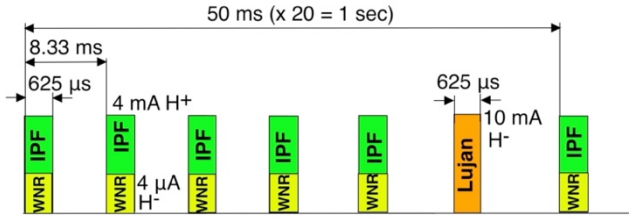

Figure 2: Layout of Lujan/WNR/IPF beams. Beams delivered to pRad or UCN facilities, "steal" their time cycles from WNR beam.

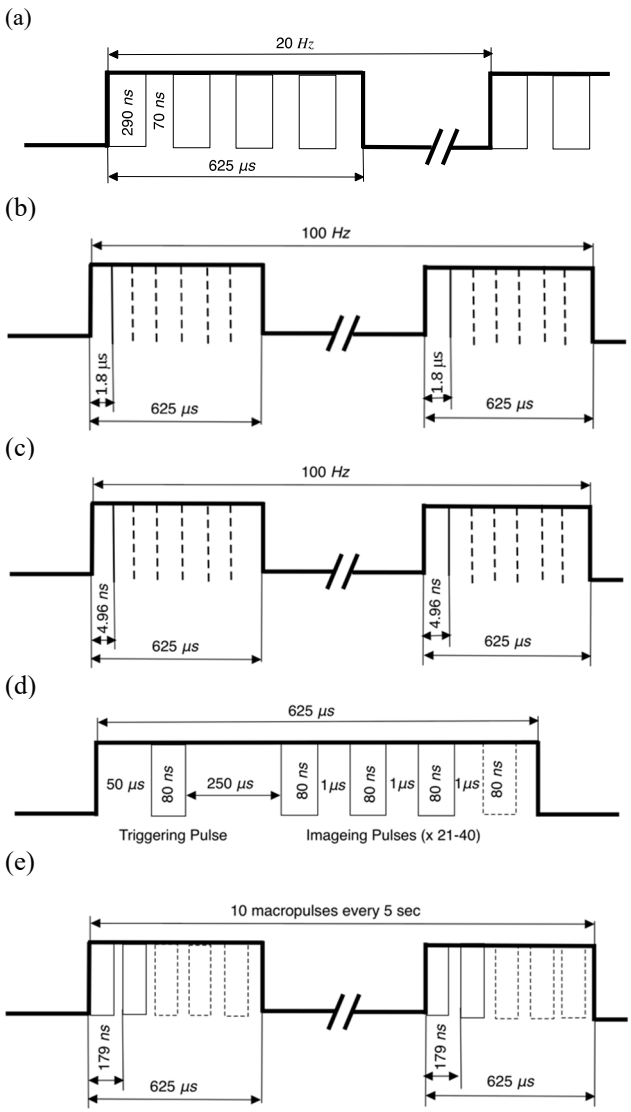

Figure 3: Time structure of LANSCE beams: (a) Lujan-PSR, (b) Weapons Neutron Research Facility, (c) Isotope Production Facility, (d) Proton Radiography Facility, (e) Ultra Cold Neutron Facility. Vertical dotted lines illustrate single bunches.

interval of 290 ns every 358 ns, which is the revolution time for the Proton Storage Ring. After accumulation, the beam is extracted to the moderated neutron spallation target at the Lujan Center. The 70-ns gap allows for extraction and injection of the beam.

Another H^- beam, delivered to the Weapons Neutron Research Facility (WNR), shares the same 100-Hz x 625 µs pulses (that is, both beams are accelerated simultaneously) with the 100-MeV proton beam, delivered to the Isotope Production Facility. The WNR beam is a sequence of single 201.25 MHz bunches, separated by the time interval of 1.8 µs within the standard 625-µs macro-pulse (see Fig. 3b). The WNR bunch is created by the combination of a short 36 ns chopper pulse and the 16.77 MHz Low-Frequency Buncher. Because of that specific combination, the WNR bunches typically contain about 2.5 times more charge than the standard H^- linac bunch.

The IPF proton beam is a sequence of 201.25 MHz bunches separated by an RF period of 4.96 ns accelerated within the 625-µs macro-pulse (see Figure 3c). This beam has an average current of 250 µA and energy of 100 MeV, corresponding to an average beam power of 25 kW delivered to the IPF target.

H^- beam is delivered to the Proton Radiography Facility by "stealing" single 625 µs macro-pulses of H^- beam from WNR. A typical pRad structure consists of a triggering pulse followed closely by a sequence of short (80 ns) pulses separated by a time interval 1 µs for radiographic imaging (see Fig. 3d).

H^- beam is delivered to the Ultra Cold Neutron (UCN) research facility and it consumes 10 Hz x 625 µs every 5 sec, which is approximately equivalent to 2 Hz of continuous operation (see Fig. 3e). The UCN beam "steals" these cycles from WNR beam.

Simultaneous acceleration of the beams with different currents, emittance, and charge per bunch results in unavoidable beam mismatch with the accelerator structure. The initial tune-up of the accelerator is performed for the most powerful 80-kW H^- beam delivered to the Lujan Center. Subsequent fine-tuning for all beams is provided to achieve a reasonable level of beam loss for all the beams. Details of beam tuning are presented in Ref. [2].

BEAM EMITTANCE GROWTH AND BEAM LOSS

Achievable beam power in the LANSCE accelerator is limited by CCL klystrons power and level of beam losses. The optimal operation of the accelerator facility critically depends on the emittance and brightness of the beam extracted from the ion sources and beam formation in the low-energy beam end. The H^+ beam injector operates with the duoplasmatron proton source (see Fig. 4a) which delivers a high-brightness beam with a current I = 10 - 30 mA and normalized rms emittance ε_{rms} = 0.003 – 0.005 π cm mrad [3]. The H^- beam injector is based on a cesiated, multicusp - field surface-production ion source (see Fig. 4b) with beam current I = 14 - 16 mA, and normalized emittance ε_{rms} = 0.018 π cm mrad [4].

Beam emittance is measured using the slit-collector method at the Front End up to the energy of 100 MeV. There are seven beam emittance measurement stations in the low-energy beam transports and three stations after the 100 MeV Drift Tube Linac. At the high-energy part of the

ISBN: 978-3-95450-253-0 ISSN: 2673-5571 doi:10.18429/JACoW-HB2023-TUC1I1

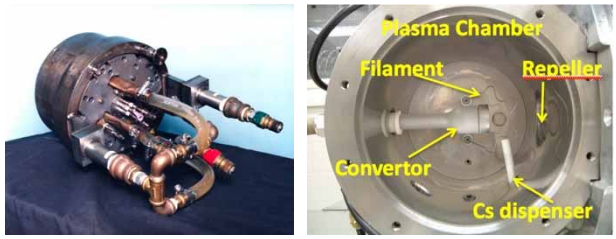

Figure 4: (a) duoplasmatron proton source, (b) cesiated, multicusp-field, surface production H- ion source.

linac, the 800-MeV beam emittance is measured using a combination of wire scanners, with the calculation of emittance using a matrix method.

While the accelerator facility delivers beams to 5 targets, there are 3 types of beams with different emittances and different charges per bunch. During acceleration, the beams experience emittance growth. Table 2 illustrates the emittance growth of various beams in the LANSCE accelerator, including a high-power 800 kW H^+ beam delivered to Area A until 1999. Significant emittance growth due to intrinsic beam mismatch is observed in DTL, especially in H^- beam transported to WNR, and H^+ beam transported to IPF. Figure 5 illustrates initial emittance growth in 750-keV LEBTs due to RF beam bunching, and Figure 6 illustrates that due to beam chopping.

Another metric of beam quality is beam loss. The typical distribution of beam losses along the accelerator facility is presented at Figure 7. Total averaged beam losses along CCL accelerator are 2 x 10^{-3} which corresponds to a loss rate of 3 x10^{-6} m^{-1}, or 0.2 W/m. At the time of operation of the accelerator as an 800-kW continuous proton beam power, the relative average beam losses generated by the proton beam with an average current of 1 mA were at the level of ~ 5·10^{-7} m^{-1} [5]. While the present power of the most powerful 800-kW H^- beam is an order of magnitude smaller than that of the 800-kW proton beam in the previous operation, the losses and activation from both beams are comparable. It is explained by the fact that the rate of beam loss of the H^- beam is an order of magnitude larger than that of H^+ beam [6] due to the presence of several stripping mechanisms in negatively charged ions.

Beam loss of 3.6 kW WNR H^- beam is at the level of 25% of that generated by the 80 kW H^- beam directed to PSR and extracted to reach the 1L Target of Lujan Neutron Scattering Center. Therefore, the specific beam loss generated by a WNR bunch is ~ 5.5 larger than that in the Lujan/PSR beam. Since the charge of the WNR bunch is 2.5 larger than that of the Lujan/PSR bunch, the loss in H^- beam is approximately proportional to the square of the bunch population. Such dependence is typical for intra-beam stripping mechanism in H^- beams [7].

Table 2: Normalized Transverse RMS Beam Emittance (π cm mrad) and Charge Per Bunch (Q/b) in Linac

Beam (Facility)	Source	0.75 MeV	100 MeV	800 MeV	Q/b pC
H (Luj/ pRad/UCN)	0.018	0.022	0.045	0.07	50
H^- (WNR)	0.018	0.027	0.058	0.124	125
H^+ (IPF), DTL only	0.003	0.005	0.026		20
H^+ (Area A, 1995)	0.005	0.008	0.030	0.07	82

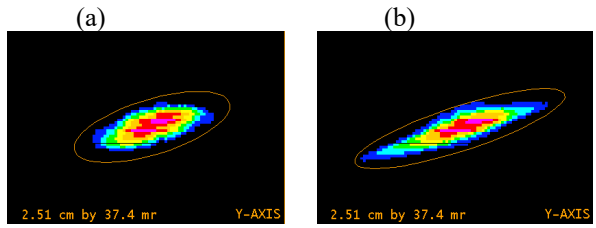

Figure 5: Effect of 750 – keV H^- Lujan beam bunching on beam emittance: (a) buncher off, (b) buncher on.

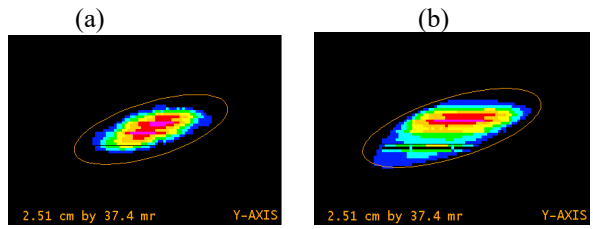

Figure 6: Effect of H^- WNR beam chopping on beam emittance: (a) chopper off, (b) chopper pulse 36 ns.

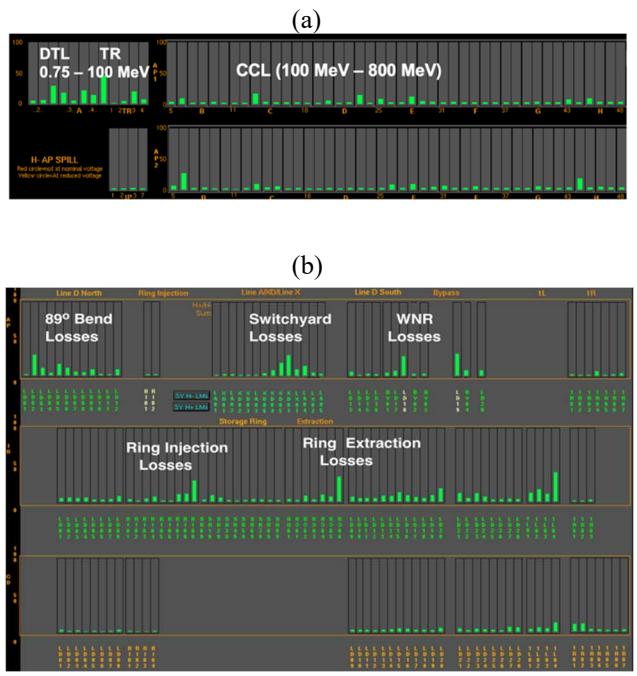

Figure 7: EPICS display of beam loss in (a) linear accelerator, (b) in high-energy ream transport.

ISBN: 978-3-95450-253-0 ISSN: 2673-5571 doi:10.18429/JACoW-HB2023-TUC1I1

Table 3: Effect of Various Sources on Beam Emittance Growth and Beam Loss in Linac: (Red) Significant, (Yellow) Moderate, (Green) Insignificant

Source	0.75 MeV LEBT	100 MeV DTL	800 MeV CCL	800 MeV HEBT
Lattice misalignments	●	●	●	No data
Transv.-longitudinal coupling	●	●	●	N/A
H- beam stripping	●	●	●	●
Lattice field nonlinearities	●	●	●	●
Beam space charge	●	●	●	●
Beam mismatch	●	●	●	●
Lattice field instabilities	●	●	●	●
Beam energy tails	●	●	●	●
Un-chopped (dark) current	●	●	●	●
Higher order RF modes	●	●	●	N/A

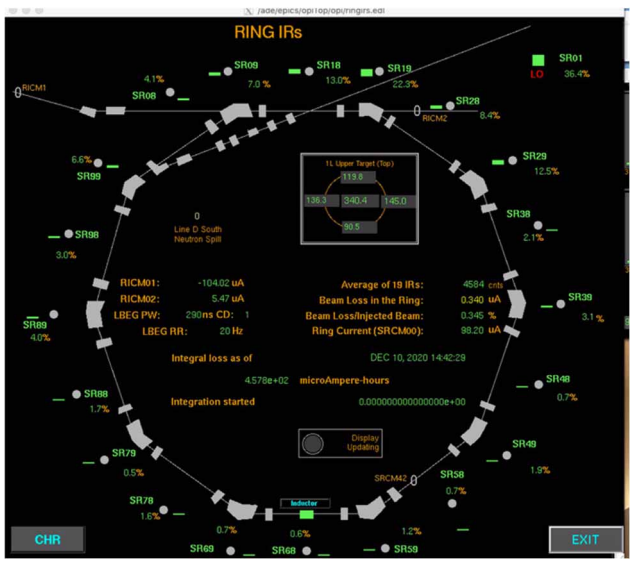

Figure 8: Distribution of beam losses in 800-MeV Proton Storage Ring.

In high-energy beamlines, the beam loss rate is 2 x10^{-5} m^{-1}, or 1.6 W/m. Larger beam loss rate in HEBT is explained by the dispersive nature of beamlines, which generates additional losses due to longitudinal beam tails and energy tails.

PSR is the 90-m circumference storage ring, accumulating ~ 5 μC of protons within 625 μs and extracting it to the 1L target within 290 ns. Typical average losses in the Proton Storage Ring are at the level of 0.3% (see Fig. 8). Sources and optimization of beam loss in PSR are discussed in detail in Ref. [8].

Table 3 illustrates the main sources of beam emittance growth and beam loss in the LANSCE linear accelerator. The primary causes of beam degradation are space-charge forces of the beam, mismatch of the beam with accelerator structure, instabilities of accelerating and focusing field, beam energy tails from uncaptured particles, and H- intra beam stripping. One of the main sources of beam degradation is strong oscillations of the mismatched beam envelopes along the CCL accelerator due to the doubling of the focusing period at the energy of 211 MeV, while quadrupole gradients are kept at the same level (see Fig. 9). This is a result of the initial design of the accelerating-focusing lattice. The matching of the beam with the accelerator requires redesigning the quadrupole structure of the accelerator.

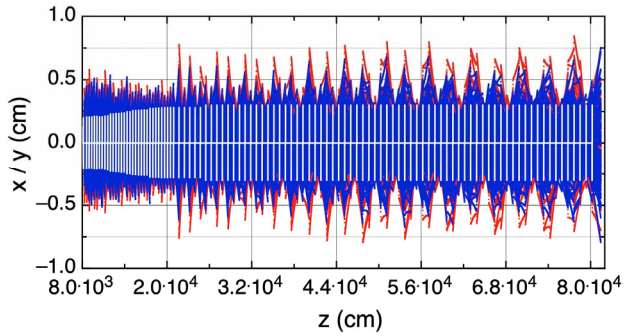

Figure 9: (red, blue) particle trajectories in the Coupled Cavity Linac, (white) gradients of quadrupole lenses.

EFFECT OF LATTICE MISALIGNMENT AND RF FIELD VARIATION

Accelerator channel misalignments in a long linear accelerator is one of the factors, affecting beam parameters. Laser tracker measurement of the LANSCE lattice misalignments was performed by the Mechanical Design Engineering Group of the Los Alamos Accelerator Operations and Technology Division (see Fig. 10) [9]. Measured data were translated into transverse displacement and slopes of each accelerating tank, and displacement of quadrupole doublets between tanks (see Fig. 11). Results of measurements indicate significant deviation of axes of accelerator in *x*- and *y*- directions with random variation of positions of accelerating and focusing elements around an axis.

The misalignment data in DTL are limited because the positions of quadrupole lenses inside drift tubes are unavailable. The numerical study of the effect of misalignment was performed in high-energy Coupled Cavity Linac. Modeling was performed taking into account displacements and tilts of accelerating tanks, displacements of quadrupole lenses including 6-th order quadrupole field component, and measurement data on RF field gradients in tanks (see Fig. 12).

Simulations show that the contribution of misalignment in relative beam emittance growth based on available measured data is around 10%, while other factors (space charge, RF amplitude beam distortion) have a comparable or larger effect on beam emittance (see Fig. 13). Accomplished simulation shows that misalignments are not the major sources of reducing beam quality, and the alignment of the accelerator is not expected to provide significant improvement in beam characteristics.

ISBN: 978-3-95450-253-0 ISSN: 2673-5571 doi:10.18429/JACoW-HB2023-TUC1I1

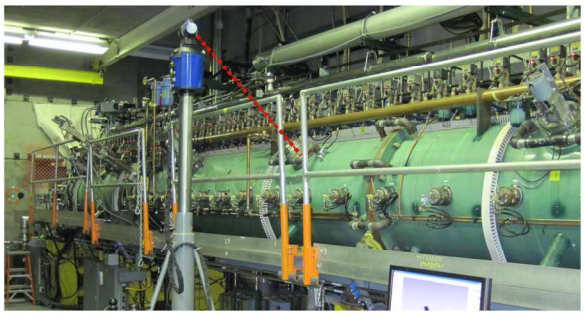

Figure 10: Laser tracker measurement of lattice misalignment in Drift Tube Linac.

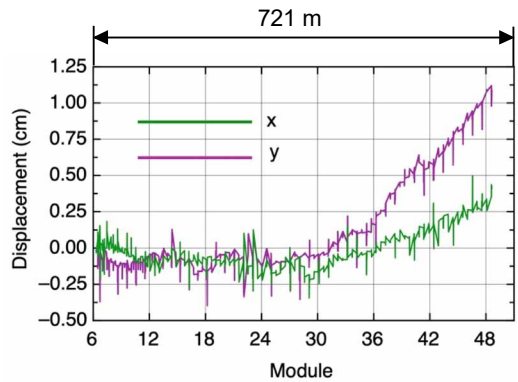

Figure 11: 805 MHz CCL misalignment data.

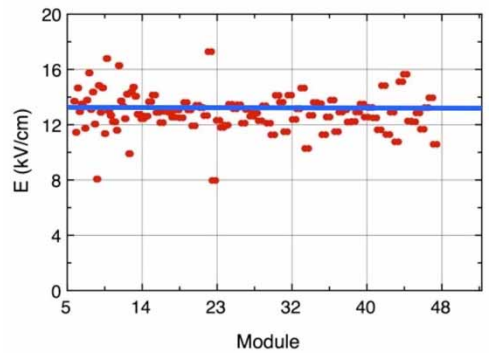

Figure 12: RF field amplitude variation in CCL accelerating modules; (blue) - design.

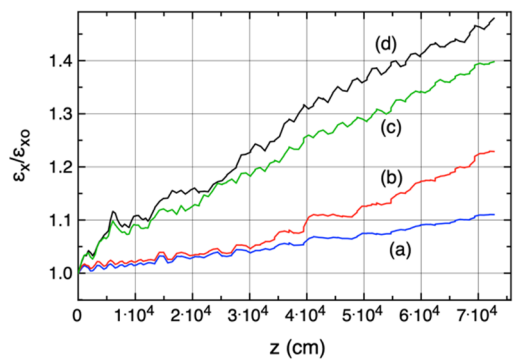

Figure 13: Beam emittance growth along CCL linac: (a) ideal structure, (b) structure with misalignment, (c) structure with misalignment, and beam space charge, (d) structure with misalignments, beam space charge, and RF field variation.

MITIGATION OF BEAM LOSS

Suppression of beam losses is essential for the successful operation of a high-intensity accelerator facility. Multiple beam development experiments were performed to reduce emittance growth and beam loss. Significant reduction of the beam emittance growth and beam loss in the Front End of the accelerator were achieved with:

- Maximization of beam brightness of the proton ion source through adjustment of beam perveance with respect to Child- Langmuir perveance [10].
- Beam-based alignment in 750-keV proton beam transport and in 100-MeV Isotope Production Facility beamline [11].
- Application of beam tune procedure based on experimental data of space charge neutralization of the H^- beam in LEBT [12].

The serious factors limiting the achieved beam power in the LANSCE accelerator are energy tails and longitudinal beam halo in linac due to the longitudinal mismatch of the beam in front of CCL. Because of the dispersive nature of the High Energy Beam Transports after the Switchyard, such tails are converted into beam losses. Figure 14 illustrates the placement of one of the multiple phosphor screens in the 800 MeV beamlines area and the observable low-momentum beam spill. Mitigation of beam losses due to longitudinal tails (see Fig. 15) was achieved with the application of phase scans and energy scans in the tuning of CCL instead of the traditional delta-t tuning procedure, and experimental adjustment of amplitudes and phases of Drift Tube Linac and CCL [13].

FUTURE PLANS AND PROPOSED LANSCE UPGRADES

The long-term plans for the LANSCE accelerator facility assume operation of the accelerator until 2050 with significant enhancement of experimental capabilities [14]. The plans include:

- Restoration of 1-MW proton beam delivery to experimental Area A for Fusion Prototypic Neutron Source to serve as a testbed for scientific understanding of material degradation in future nuclear fusion reactors [15].
- Development of the “Neutron Target” concept for direct neutron-induced reaction studies in short-lived isotopes [16].
- Significant (~ 100X) increase of UCN beam current to improve the physics reach of the facility [17].
- Enhancement of Proton Radiography energy up to 3-5 GeV to increase imaging resolutions by an order of magnitude [18].
- Development of low-power (800 MeV x 100 nA) proton beam capability to support the demand for protons from the global security and civilian radiation effects community [19].

ISBN: 978-3-95450-253-0 ISSN: 2673-5571 doi:10.18429/JACoW-HB2023-TUC1I1

(a)

(b)

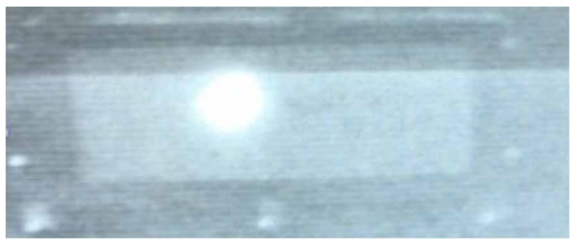

Figure 14: (a) phosphor screen in 800 MeV beamline and (b) detection of low-momentum beam spill at the screen.

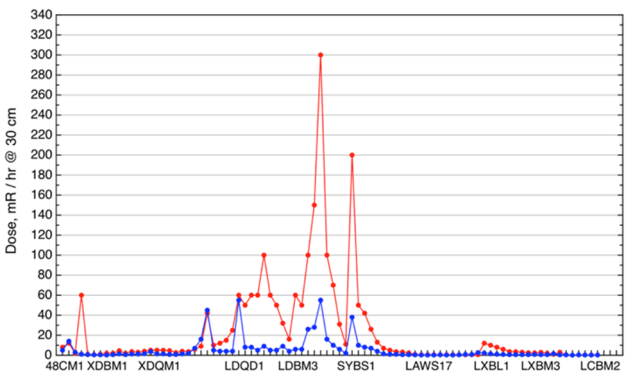

Figure 15: Switchyard radiation survey: (red) after delta-t tune, (blue) after phase-energy scans tune.

The near-term upgrade plans of LANSCE include the development of a novel 100-MeV Front End including a high-brightness Radio-Frequency Quadrupole (RFQ) based injector (see Fig. 16) and modern Drift Tube Linac [20]. The low-energy injector concept includes two independent transports merging H^+ and H^- beams at the entrance of RFQ. Beamlines are aimed to perform preliminary beam bunching in front of the accelerator section with the subsequent simultaneous acceleration of two different beams in a single RFQ. The 3 MeV injector is followed by a 100 MeV novel Drift Tube Linac, consisting of 6 tanks.

Additional improvement of beam quality in LANSCE linac can be achieved with the development of a new focusing structure of CCL accelerator and longitudinal beam matching. Six-dimensional beam matching assumes adjustments of beam phase spaces in front of DTL and CCL with an appropriate orientation of beam ellipses in 6D phase space. Existing diagnostics allow us to perform longitudinal beam matching in front of DTL, and transverse beam matching along the linac. However, longitudinal beam matching to CCL is not possible. Installation of an additional RF section before CCL is required to perform longitudinal beam matching to CCL together with novel beam diagnostics It will reduce beam losses and prevent the formation of low-momentum particle tails in the high-energy part of the linac.

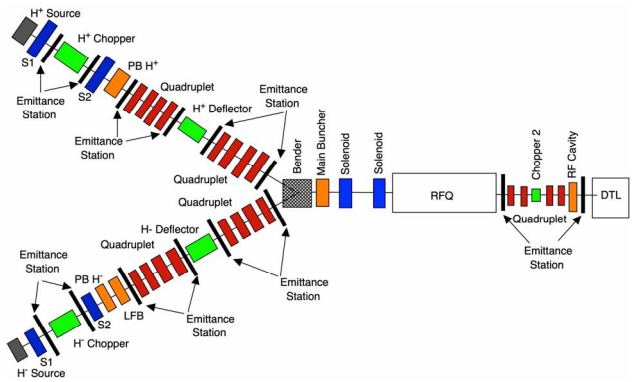

Figure 16: Layout of the proposed LANSCE RFQ-based injector.

SUMMARY

LANSCE is the unique accelerator facility, that simultaneously delivers beams to five experimental areas. Multi-beam operation of the accelerator facility requires careful optimization of beam losses, which is achieved by precise tuning of the beam in each section of the accelerator facility, imposing restriction on amplitudes and phases of RF sections, application of beam-based alignment, control of H^- beam stripping, optimization of ion sources performance and low-energy beam transport operation under space-charge neutralization. The new multi-beam 100-MeV Front End for the LANSCE accelerator facility is proposed to replace the existing LANSCE linac from the beam sources through the end of the present Drift Tube Linac.

REFERENCES

[1] P. W. Lisowski and K. W. Jones, "Status of The Los Alamos Neutron Science Center and plans for the future", in *Proc. LINAC'02*, Gyeongju, Korea, Aug. 2002, paper TU433, pp. 386-388.

[2] L. Rybarcyk, "High power operational experience with the LANSCE Linac", in *Proc. HB'08*, Nashvillle, TN, USA, Aug. 2008, paper WGD05, pp.348-352.

[3] R. R. Stevens Jr, E. P. Chamberlin, R. W. Hamm, J. R. McConnell, and R. L. York, "Injector operations at LAMPF", in *Proc. LINAC'79*, Montauk, NY, USA, Sep. 1979, paper S8-13, pp. 465-468.

[4] J. Sherman *et al.*, "Physical insights and test stand results for the LANSCE H^- surface converter source," *AIP Conf. Proc.*, vol. 763, pp. 254-266, 2005. doi:10.1063/1.1908301

ISBN: 978-3-95450-253-0 ISSN: 2673-5571 doi:10.18429/JACoW-HB2023-TUC1I1

[5] R. A. Hardekopf "Beam loss and activation in LANSCE and SNS", in *Proc. 7th ICFA Mini-Workshop on High-Intensity High Brightness Hadron Beam (Beam Halo and Scrapping)*, Eds. N.V. Mokhov and W. Chou, Lake Como, WI, USA, p. 62, 1999.

[6] L. Rybarcyk, "Characterizing and controlling beam losses at the LANSCE facility", in *Proc. HB'12*, Beijing, China, Sep. 2012, paper TUO3C03, pp. 324-328.

[7] V. A. Lebedev, N. Solyak, J.-F. Ostiguy, A. Alexandrov, and A. Shishlo, "Intrabeam stripping in H- linacs", in *Proc. LINAC'10*, Tsukuba, Japan, Sep. 2010, paper THP080, pp. 929-931

[8] R. J. Macek, "PSR experience with beam losses, instabilities and space charge effects", *AIP Conf. Proc.,* vol. 448, pp.116-127, 1998. doi:10.1063/1.56765

[9] C. Conner (LANL AOT-MDE), private communication, 2015.

[10] Y. K. Batygin, I. N. Draganic, and C. M. Fortgang, "Experimental optimization of beam quality extracted from a duoplasmatron proton ion source", *Rev. Sci. Instrum.,* vol. 85, p. 103301, 2014. doi:10.1063/1.4897150

[11] Y.K. Batygin, "Optimization of LANSCE proton beam performance for isotope production", *Nucl. Instrum. Methods Phys. Res., Sect. A*, vol. 916, pp. 8-21, 2019. doi:10.1016/j.nima.2018.10.071

[12] Y.K. Batygin, "Experimental improvement of 750-keV H– beam transport at LANSCE Accelerator Facility", *Nucl. Instrum. Methods Phys. Res., Sect. A,* yol. 904, pp. 64–73, 2018. doi:10.1016/j.nima.2018.06.054

[13] Y. K. Batygin, F. E. Shelley, and H. A. Watkins "Tuning of LANSCE 805-MHz high-energy linear accelerator with reduced beam losses", *Nucl. Instrum. Methods Phys. Res., Sect. A*, vol. 916, pp. 215-225, 2019. doi:10.1016/j.nima.2018.11.103

[14] C. Sinnis, M. B. Chadwick, K. C. N. Scott, and S. V. Milton, "LANSCE 21st Century Deterrence", Los Alamos National Laboratory, NM, USA, LANL Rep. LA-UR-20-22771, 2020.

[15] E. J. Pitcher, Y. K. Batygin, and S. A. Maloy, Los Alamos National Laboratory, NM, USA, LANL Rep. LA-UR-19-32216, 2019.

[16] S. Mosby *et al*., "Status and prospects for the development of a Neutron Target Facility", Los Alamos National Laboratory, NM, USA, LANL Rep. LA-UR-21-30261, 2021.

[17] K. Leung *et al*., "A next-generation inverse-geometry spallation-driven ultracold neutron source", *J. Appl. Phys.*, vol. 126, no. 22, p. 224901, 2019. doi:10.1063/1.5109879

[18] Y. K. Batygin and S. S. Kurennoy, "Design of 3-GeV high-gradient booster for upgraded proton radiography at LANSCE", in *Proc. NAPAC'22*, Albuquerque, NM, USA, Aug. 2022, pp. 891-893. doi:1018429/JACoW-NAPAC2022-TUPA48

[19] S. A. Wender, D. Tupa, E. Guardincerri, and Y. K. Batygin, "Development of Low-Power Proton Beam Capability in Area-A", Los Alamos National Laboratory, NM, USA, LANL Rep. LA-UR-23-23298, 2023.

[20] Y. K. Batygin, D. A. D. Dimitrov, I. Dragani, D. V. Gorelov, E. Henestroza, and S. S. Kurennoy, "High-Brightness RFQ Injector for LANSCE Multi-Beam Operation", in *Proc. LINAC'22*, Liverpool, UK, Aug.-Sep. 2022, pp. 130-133. doi:10.18429/JACoW-LINAC2022-MOPOPA24